Cell Stem Cell
Article

Tissue Damage-Induced Intestinal Stem Cell Division in *Drosophila*

Alla Amcheslavsky,[1] Jin Jiang,[4] and Y. Tony Ip[1,2,3,*]
[1]Program in Molecular Medicine
[2]Program in Cell Dynamics
[3]Department of Cell Biology
University of Massachusetts Medical School, Worcester, MA 01605, USA
[4]Center for Developmental Biology, University of Texas Southwestern Medical Center, Dallas, TX 75390, USA
*Correspondence: tony.ip@umassmed.edu
DOI 10.1016/j.stem.2008.10.016

SUMMARY

Stem cell division is essential for tissue integrity during growth, aging, and pathogenic assaults. Adult gastrointestinal tract encounters numerous stimulations, and impaired tissue regeneration may lead to inflammatory diseases and cancer. Intestinal stem cells in adult *Drosophila* have recently been identified and shown to replenish the various cell types within the midgut. However, it is not known whether these intestinal stem cells can respond to environmental challenges. By feeding dextran sulfate sodium and bleomycin to flies and by expressing apoptotic proteins, we show that *Drosophila* intestinal stem cells can increase the rate of division in response to tissue damage. Moreover, if tissue damage results in epithelial cell loss, the newly formed enteroblasts can differentiate into mature epithelial cells. By using this newly established system of intestinal stem cell proliferation and tissue regeneration, we find that the insulin receptor signaling pathway is required for intestinal stem cell division.

INTRODUCTION

Tissue homeostasis requires the balance between removing dead cells and producing new cells. Replenishment of lost cells is likely mediated by adult stem cells residing within an individual tissue (Nystul and Spradling, 2006; Metcalfe and Ferguson, 2008; Niemeyer et al., 2006). In adult mammalian intestine, stem cells are located near the base of each crypt (Crosnier et al., 2006; Walker and Stappenbeck, 2008; Yen and Wright, 2006). These intestinal stem cells (ISC) divide to form progenitor cells in the transit amplifying zone, providing larger number of precursor cells that can replenish cells of various lineages. Wnt, BMP, and Notch signaling pathways, e.g., have been shown to play important roles in mammalian intestinal cell proliferation (Fodde and Brabletz, 2007; Nakamura et al., 2007). However, specific markers for mammalian ISC remain rare, the exact identity of the stem cells is still arguable, and the regulation of stem cell division in response to environmental challenge is largely unknown (Barker et al., 2007; Demidov et al., 2007; He et al., 2007; Scoville et al., 2008; Sangiorgi and Capecchi, 2008).

In adult *Drosophila* midgut, the mature enterocytes of the entire epithelium are replaced in approximately 1 week (Micchelli and Perrimon, 2006). There are many ISC in *Drosophila* midgut, and they are distributed evenly underneath the enterocytes (Micchelli and Perrimon, 2006; Ohlstein and Spradling, 2006). When an ISC divides, it gives rise to two cells, with one retaining stem cell properties and the other becoming an enteroblast. Enteroblasts are precursors that do not divide any more but can differentiate along two lineages to become enterocytes or enteroendocrine cells (see Figure 1C). Approximately ninety percent of the enteroblasts will become enterocytes, and ten percent will become enteroendocrine cells (Ohlstein and Spradling, 2007).

Cell-fate determination between the two daughter cells after ISC division requires Delta and Notch (Micchelli and Perrimon, 2006; Ohlstein and Spradling, 2007). Active Delta, detected as punctate cytoplasmic staining (Bray, 2006), is so far the only known specific marker for *Drosophila* ISC. Immediately after ISC division, higher level of active Delta is retained in the cell that remains as ISC. The newly formed, neighboring enteroblast quickly loses the active Delta. This asymmetric level of active Delta causes stimulation of the Notch signaling pathway in the newly formed enteroblast. Depending on the level of Delta in the ISC, stimulation of Notch in the enteroblast may direct the differentiation along the enterocyte lineage or the enteroendocrine cell lineage (Ohlstein and Spradling, 2007).

It is not known whether the midgut ISC have constant division cycle or can vary their division rate according to the need, such as during injury or aging. To address this question, we examined whether *Drosophila* adult ISC division can be regulated by tissue damage. By feeding tissue-damaging agents and expressing apoptotic proteins, we show that epithelial injury can increase ISC division. Furthermore, if the damage leads to epithelial cell loss, the newly divided enteroblasts can differentiate faster into mature enterocytes. These results together support the idea that epithelial damage can stimulate the underlying ISC to divide more for tissue repair. We used this newly established system to show that the insulin receptor signaling pathway is critical for ISC division.

RESULTS

Feeding of Dextran Sulfate Sodium Causes Midgut Cell Proliferation

When included in drinking water, dextran sulfate sodium (DSS) causes injury in the intestines of experimental mammals, and

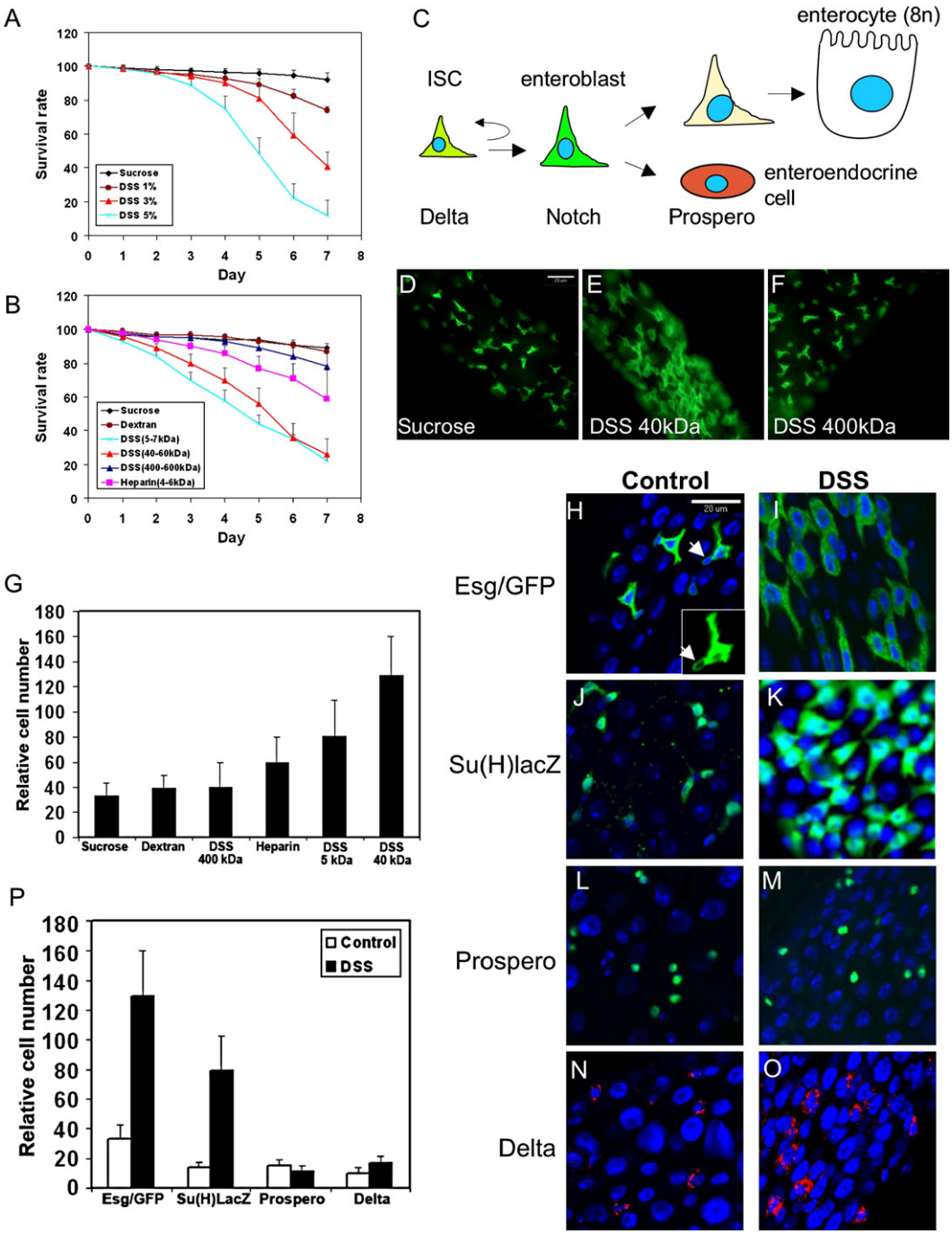

Figure 1. DSS Feeding Causes Mortality and Increases Enteroblast Number

(A) Various amounts of DSS as indicated were included in the sucrose feeding medium, and the percentage of flies alive after each day is expressed as survival rate. The inclusion of DSS causes increased mortality.

(B) 3% of each of the indicated polysaccharides was included in the feeding medium, and the flies were counted each day. High molecular weight DSS and dextran do not significantly change the viability of the flies, while low molecular weight DSS does.

(C) An illustration of the cell types and differentiation pathways in adult midgut.

(D–F) Cell proliferation effect revealed by the esg-Gal4/UAS-CD8GFP marker. The type of polysaccharide used is indicated in the lower right corner of each panel. The scale bar shown in (D) is 20 μm.

(G) Quantification of esg-Gal4/UAS-CD8GFP-positive cells after feeding with various polysaccharides as indicated. The number of GFP-positive cells were counted in multiple images for each experiment and normalized by 100 unstained cells as revealed by DAPI staining. The error bar is standard deviation.

(H–O) The blue color in these panels and all other figures is DAPI staining of DNA. The red or green staining is for the antigens indicated to the left. The left columns are control gut staining, and the right columns are stained guts from DSS-fed flies. The DSS feeding experiments were performed with 3% of 40 kDa DSS for 2 days at 29°C unless specified. The arrowhead in (H) indicates an ISC.

complex interactions in the gut milieu lead to excessive inflammation resembling ulcerative colitis in humans (Kawada et al., 2007; Rakoff-Nahoum et al., 2004; Tlaskalova-Hogenova et al., 2005). We tested the idea that DSS could cause similar tissue damage in adult *Drosophila* gut. When the feeding sucrose solution contained 5% of DSS (average MW 40 kDa), approximately 50% of the flies died within 5 days (Figure 1A). Together with the killing curves of 1% and 3% DSS, we show that there is a dose-dependent killing of flies by DSS. We also tested related polysaccharides and found that feeding sucrose solution containing 3% of 400 kDa DSS or dextran (a nonsulfated polysaccharide) did not significantly change the viability of the flies (Figure 1B). Heparin, another sulfated polysaccharide, had an intermediate effect, while 5 kDa DSS also caused significantly increased lethality.

The *escargot*-promoter-driven Gal4 expression (esg-Gal4) (Micchelli and Perrimon, 2006), when crossed with the UAS-CD8GFP, can mark both ISC and enteroblasts in adult *Drosophila* midgut (Figure 1C). We used these flies for feeding experiments with 3% of the various polysaccharides in the sucrose solution for 2 days. We found that the 5 and 40 kDa DSS caused a significant increase in the number of GFP-positive cells, while the 400 kDa DSS and dextran did not induce a gut phenotype (Figures 1D–1G). The 40 kDa DSS is the most commonly used reagent in mammalian experiments, and the effect in *Drosophila* gut was highly reproducible, as 84.3% (n = 51) of the DSS fed-samples and 0% (n = 52) of control samples showed the cell proliferation phenotype. A correlation between the killing effect and cell proliferation phenotype by the various polysaccharides is also apparent.

DSS Feeding Increases the Number of Enteroblasts

The esg-Gal4/UAS-CD8GFP marks both ISC and enteroblasts. After costaining with Delta (data not shown; Micchelli and Perrimon, 2006; Ohlstein and Spradling, 2007), we confirm that the ISC is usually the one with a lower level of GFP signal and a more rounded cell shape (Figure 1H, arrowhead, insert). After DSS feeding, most of the GFP-positive cells appeared to be of bigger size with a strong GFP signal (Figure 1I). We next examined the maker Su(H)Gbe-lacZ, which is a Notch pathway target gene and is specific for enteroblasts (Micchelli and Perrimon, 2006; Ohlstein and Spradling, 2007). The staining showed that there were clearly more β-galactosidase-expressing cells after DSS treatment (Figures 1J and 1K).

Prospero is a homeodomain protein that is expressed specifically in enteroendocrine cells (Micchelli and Perrimon, 2006). The Prospero staining showed no apparent increase in the number of enteroendocrine cells (Figures 1L and 1M). Meanwhile, punctate Delta staining in cytoplasm represents the only known ISC-specific marker (Ohlstein and Spradling, 2007). In control samples, low levels of punctate Delta could be detected in cells with small nuclei, suggesting that they are ISC. In DSS-treated guts, the Delta fluorescent signal became more easily detectable (Figures 1N and 1O). We counted the number of cells that expressed the different markers and, in each case, normalized with nonstained cells based on DAPI staining. The quantification indicates that the number of cells expressing esg-Gal4/UAS-CD8GFP and Su(H)Gbe-LacZ had increased by approximately 4-fold, while Delta- and Prospero-positive cell number had changed by less than 1.5-fold (Figure 1P). These results support our idea that the most prominent phenotype induced by DSS is an accumulation of enteroblasts.

Intestinal Stem Cell Division Is Increased after DSS Feeding

We surmised that DSS feeding caused an increase in ISC division, leading to the accumulation of enteroblasts. ISC is the only cell type in midgut that goes through division, while enteroblasts undergo endoreplication during differentiation into enterocytes, which are polyploid (Figure 1C). Phosphorylated-histone 3 (phospho-H3) is a highly specific marker for condensed chromosomes and, thus, can be used to assess the number of mitotic ISC. The number of phospho-H3-positive cells in dissected guts from DSS-fed flies was approximately 20-fold higher than in control samples (Figures 2A–2C). These results support our hypothesis that DSS increases ISC division. We used 3- to 5-day old flies for experiments but also noted that older flies had more mitotic cells (see also Choi et al., 2008).

We performed a series of experiments to determine the cell-fate and stem cell properties after DSS feeding. Double staining for Delta and Su(H)Gbe-lacZ revealed that there was no overlap before or after DSS feeding (Figures 2D–2I, arrows), demonstrating that ISC and enteroblast fates are preserved. By another double-staining experiment, we found that all the phospho-H3-positive cells had Delta staining (Figures 2J–2O), demonstrating that after DSS feeding, ISC retained the ability to proliferate and contained a high level of Delta. Therefore, the asymmetry, cell-fate determination, and known properties of ISC are not affected during the experimental period of DSS feeding.

We then performed the mosaic analysis with repressible cell marker (MARCM), which randomly allows Gal4-driven GFP marking of individual ISC lineage due to FLP-FRT-mediated mitotic recombination that removes the repressor Gal80 (Lee and Luo, 2001; Micchelli and Perrimon, 2006; Ohlstein and Spradling, 2006). In control guts of MARCM flies fed with sucrose, GFP expression was detected in a small number of isolated cells (Figures 2P–2R). Under the same feeding condition, the DSS-treated flies had more GFP-positive cells and were present in clusters (Figures 2S–2U). Within each cluster, only one cell exhibited punctate Delta staining (arrowhead). Each isolated cluster should represent a single lineage originated from one ISC, supporting the idea that DSS feeding increases the number of cells produced by an ISC and only one ISC is formed after each division.

DSS Disrupts Basement Membrane Organization and Does Not Induce Enteroblast Differentiation

One speculation regarding stem cell-mediated repair is that stem cell division is increased and the daughter cells should differentiate to replenish lost cells. While many enteroblasts accumulated around ISC, no similar increase in mature enterocytes was observed after DSS feeding. Phalloidin stains F-actin, which

(P) Quantification of the positively stained cells for the various markers as indicated. The relative number is presented as stain-positive cells per 100 unstained cells revealed by DAPI staining. The error bar is standard deviation.

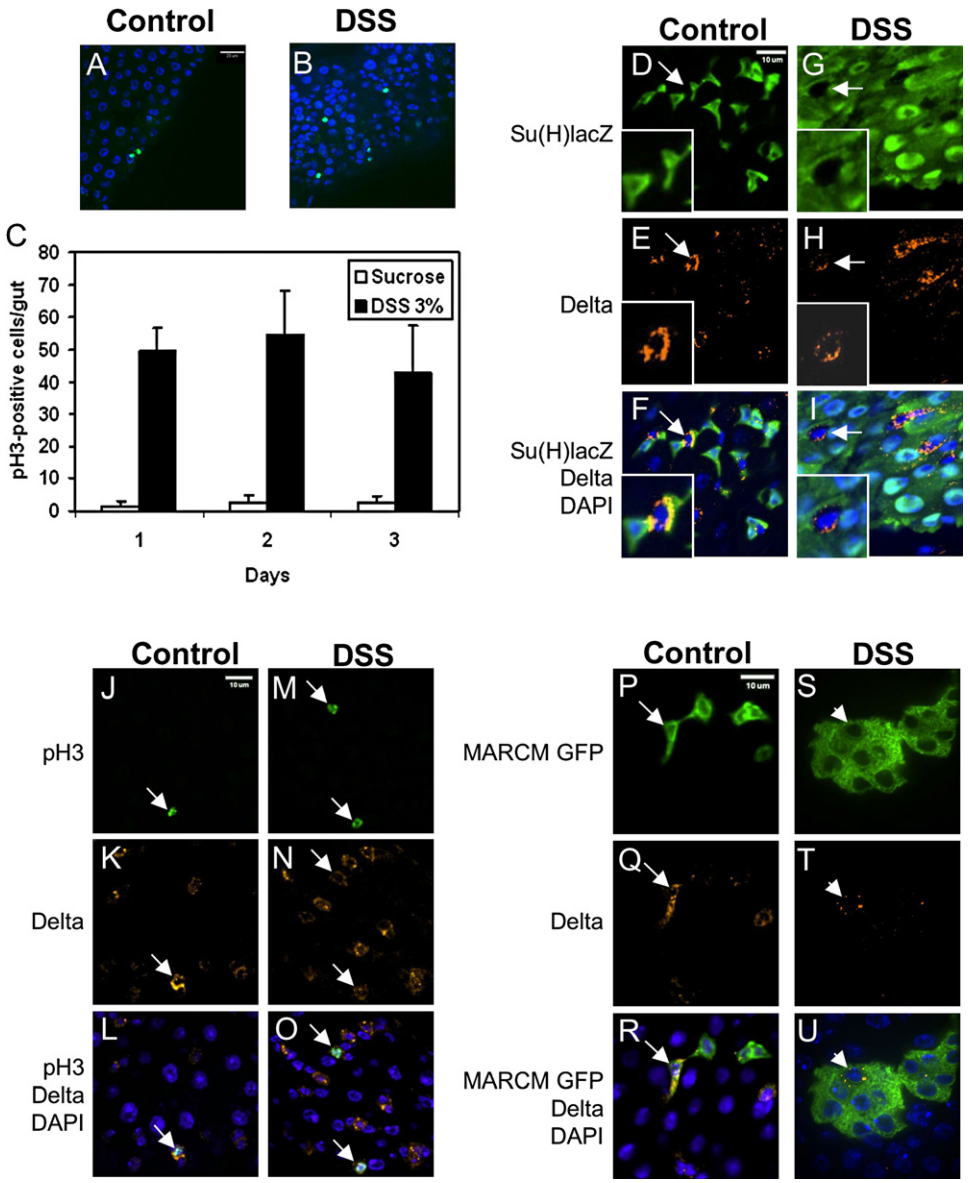

Figure 2. DSS Increases ISC Division and Does Not Affect Cell-Fate Determination

(A and B) Immunofluorescent staining using antibody against phospho-H3 is shown (green). DSS increases the number of phospho-H3-positive cells.

(C) Phospho-H3-positive cell count in whole gut, from anterior midgut next to cardia to posterior midgut before malpighian tubules. The average number per gut and standard deviation is shown.

(D–I) Green staining is anti-β-galactosidase for enteroblasts, red staining is anti-Delta for ISC, and blue staining is DAPI for DNA. 3% DSS feeding was carried out for 2 days. The arrows in control and DSS panels point to ISC with positive Delta staining but no β-galactosidase staining. The inserts are enlargements of the cells indicated by the arrows.

(J–O) Double staining for phospho-H3 (green) and Delta (red). All phospho-H3-positive cells have Delta staining (arrow), with or without DSS feeding.

(P–U) Each cluster of GFP-positive cells represent one lineage originated from one parental ISC after MARCM. All MARCM feeding experiments were performed for 14 days in 18°C. The control clones contain 1 to 2 cells. The arrow points to an ISC with Delta staining and GFP. In DSS-fed flies of similar age, the clone has grown to 7 cells in this one confocal plane. Within each cluster, almost always only one cell is Delta positive (red, indicated by arrowhead). Therefore, ISC asymmetry and renewal after DSS feeding is normal.

is present at high levels in the apical brush border of mature enterocytes and in smooth muscle cells (Micchelli and Perrimon, 2006). In both control and DSS-fed samples (Figures 3A–3F), all the MARCM GFP-expressing cells (arrowheads) had smaller nuclei, stayed closer to the basal side, and did not closely associate with phalloidin staining (arrows). This result suggests that DSS induces enteroblast accumulation but does not induce differentiation into mature enterocytes.

To gain insights into the apparent lack of stimulated differentiation, we examined the tissue injury phenotype after DSS feeding. By tissue sectioning, we found that the overall morphology of the gut appeared intact and did not exhibit extensive ulcer

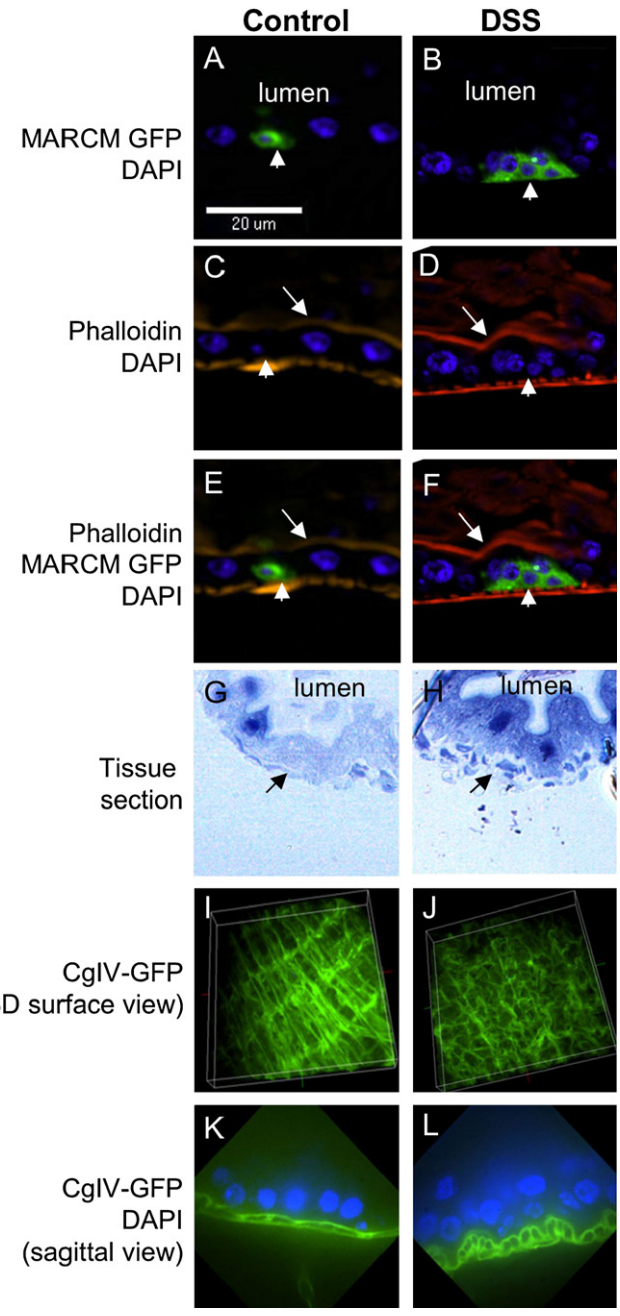

Figure 3. DSS Disrupts Basement Membrane Organization and Causes Enteroblast Accumulation

(A–F) MARCM clones are GFP positive, indicated by the arrowheads. In the DSS-fed sample, the cluster of GFP-positive cells stay close to the basal side and are not closely associated with the phalloidin staining at the apical side of bigger enterocytes (arrow). Therefore, these accumulated GFP-positive cells are enteroblasts, but not mature enterocytes. The orientation of these sagittal images is apical to the top.

(G and H) Cross-sections of gut tissue from control and DSS treated flies. The tissue sections were stained with toluidine blue. The enterocyte nuclei have dark blue staining. The lumens are indicated on the panels. The arrows point to the basal layer, which is smoother in control and discontinuous in DSS samples.

(I and J) Surface views of 3D reconstructed confocal images of guts dissected from a collagen IV-GFP fly line. In control gut, the longitudinal filaments (top to bottom direction) are connected by transverse filaments (left to right direction). This scaffolding pattern probably represents part of the basement membrane structure. In gut from DSS-fed fly, this GFP pattern is less organized, suggesting a disruption of basement membrane structure.

(K and L) Confocal sagittal views of control and DSS-treated guts from collagen IV-GFP flies. There are clear differences between the two samples: the two layers of longitudinal filaments seen in control gut become more rounded in DSS-treated gut. The orientation of the images is apical to the top.

or cell loss (Figures 3G and 3H), different from that observed in mammalian experiments (see discussion). Instead, we noticed that the basal layer underneath the enterocytes appeared broken (arrows). To further investigate this phenotype, we used a fly line expressing GFP fusion protein of collagen IV (Figure 3I), which is part of the basement membrane structure (Baba et al., 2007; LeBleu et al., 2007). Interestingly, the scaffolding pattern of collagen IV-GFP became less organized in DSS-fed samples (Figure 3J). In sagittal view of control gut, there are two layers of collagen IV-GFP signal connected by transverse filaments (Figure 3K). In DSS-treated guts, the two layers became more rounded and separated (Figure 3L). We speculate that DSS disrupts basement membrane organization, which is sensed by ISC and causes increased cell division. The lack of cell loss in the epithelial layer, however, may account for the absence of a signal required to stimulate enteroblast differentiation.

Bleomycin Feeding Causes Damage Specifically in Enterocytes

We examined other tissue-damaging agents in order to test the idea that epithelial cell loss may stimulate both ISC division and enteroblast differentiation, hallmarks of stem cell-mediated tissue repair. Bleomycin is an anticancer drug that is also widely used as a DNA-damaging agent in experimental systems (Takada et al., 2003; Morel et al., 2008). We found that feeding of bleomycin to adult flies caused lethality in a dose-dependent manner (Figure 4A). We then stained for phospho-histone 2A variant D (H2AvD), which accumulates in response to DNA damage, possibly through the protein kinase ATM (Clarkson et al., 1999; Klattenhoff et al., 2007). The control guts showed a low level nuclear punctate staining of H2AvD (Figures 4B–4D). In bleomycin-fed samples, we observed a much stronger staining associated with entire nuclei of most enterocytes (Figures 4E–4G, arrow). More importantly, no H2AvD staining was observed with small nuclei in the basal side (marked by esg-Gal4/UAS-GFP, arrowhead). These results demonstrate that bleomycin feeding causes DNA damage specifically in enterocytes. We also stained the guts for Spectrin, a membrane skeleton protein localized at the apical side of enterocytes (Figures 4H–4K). The staining revealed that after bleomycin feeding, the epithelial layer became disorganized and more enterocytes were shedding into the lumen (open arrow). Plastic tissue sectioning revealed a similar epithelial cell loss phenotype (Figures 4L and 4M). We speculate that bleomycin may not be able to diffuse through tight junction and, thus, causes damage only in enterocytes.

Bleomycin Induces ISC Division and Enteroblast Differentiation

We further show that bleomycin increases ISC division, while the midgut cell fates are normal. Phospho-H3 staining revealed that there was a substantial, dose-dependent increase in cell division (Figure 4N). We then used the Su(H)Gbe-lacZ line to perform

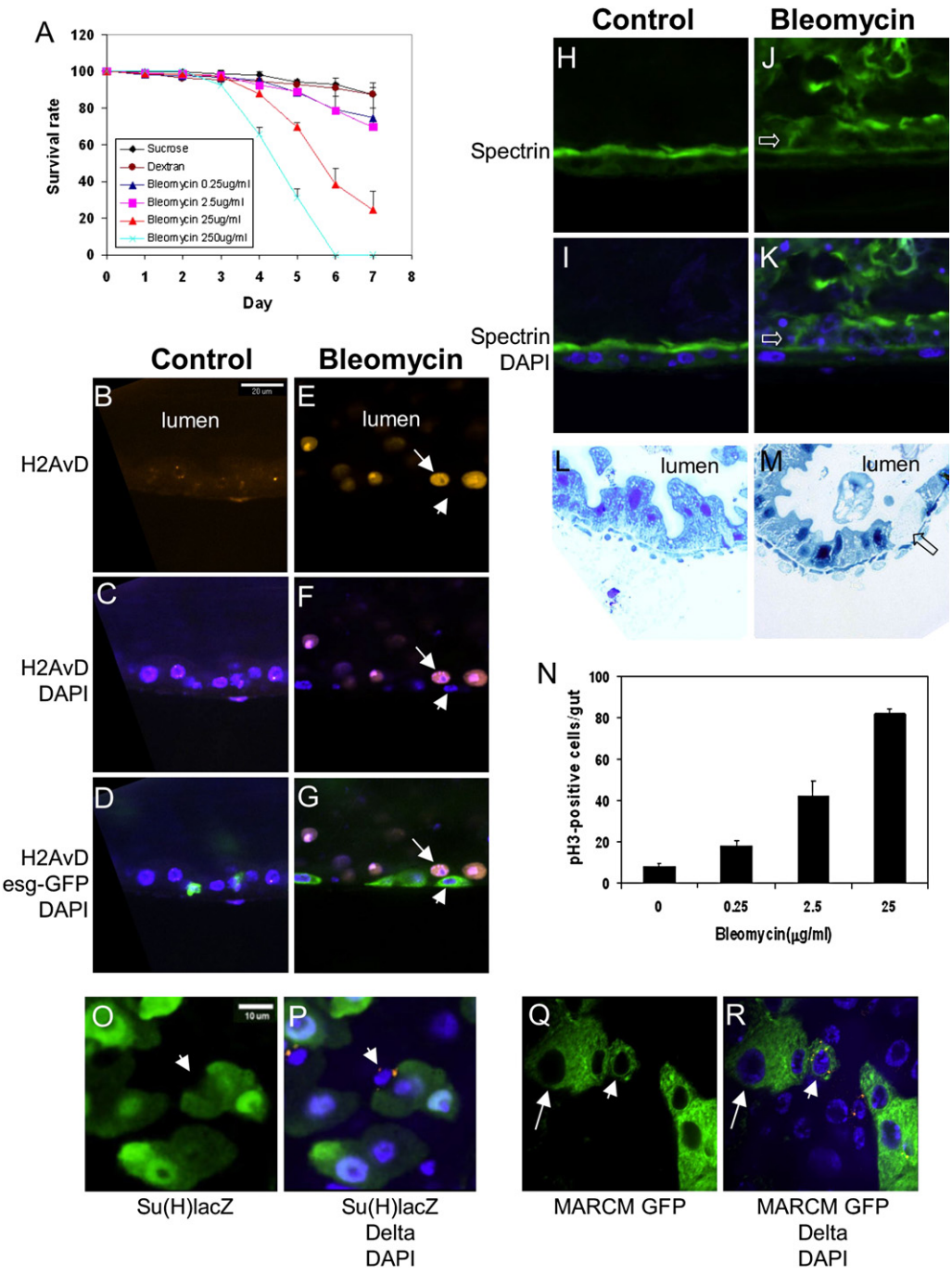

Figure 4. Bleomycin Feeding Induces Damage Specifically in Epithelial Layer

(A) Bleomycin ranges from 0.25 to 250 μg/ml or 3% dextran were included in the feeding medium. Feeding of bleomycin causes dose-dependent increase in mortality in adult flies. The error bar is standard deviation.

(B–G) DNA strand breaks are detected by anti-H2AvD staining (red). In control guts, low level of H2AvD punctate staining is colocalized with DAPI staining. The fluorescent signal is highly increased in bleomycin-treated guts, is colocalized with DAPI staining, and is only present in the bigger enterocyte nuclei (arrow). The small nuclei, marked by esg-Gal4/UASGFP expression (arrowhead), have no detectable H2AvD staining.

(H–K) Bleomycin causes epithelial layer disorganization. Spectrin (green) has higher level expression at the apical side of enterocytes. The orientation of all sagittal images is apical to the top. The open arrows indicate enterocytes that have come off the epithelial layer after bleomycin feeding.

(L and M) Plastic tissue sections show that bleomycin feeding causes falling off of some enterocytes (open arrow).

(N) Feeding experiments were performed using the indicated amount of bleomycin in the feeding medium. The number of phospho-H3-positive cells in the whole mid-gut was counted after 2 days of feeding. There is approximately 10-fold increase in ISC division after 25 μg/ml bleomycin feeding. The error bar is standard deviation.

(O and P) Double staining for Delta and Su(H)Gbe-lacZ after bleomycin feeding, 25 μg/ml for 2 days. For control, see Figure 2D. The arrowheads indicate an ISC that has a high level of punctate Delta (red) and no β-galactosidase (green).

double staining after bleomycin feeding and observed that the Delta and β-galactosidase staining were clearly distinct (Figures 4O and 4P, arrowhead). Meanwhile, the MARCM experiment showed that only one Delta-positive cell was present in each cluster (Figures 4Q and 4R, arrowhead).

One clear difference between the phenotypes induced by bleomycin versus DSS is that after bleomycin feeding, there were larger cells in each cluster (Figures 4Q and 4R, arrow). To assess whether these bigger cells are mature enterocytes, we stained MARCM samples with fluorescent-phalloidin after bleomycin feeding. In the control guts, only small cells with GFP were present (Figures 5A–5C, arrowhead). In bleomycin-fed samples, there were more GFP-positive cells, and the bigger GFP-positive cells also had tightly associated phalloidin staining at the apical side, similar to other mature enterocytes (Figures 5D–5F, arrow). In comparison, DSS induced only clusters of enteroblasts in the same period of time (Figures 5G–5I). Double feeding experiment showed that GFP-positive mature enterocytes were formed efficiently with both DSS and bleomycin in the feeding solution (Figures 5J–5L, quantification in 5M), demonstrating that DSS does not inhibit enteroblast differentiation. Overall, our data support the idea that bleomycin causes enterocyte-specific damage and cell loss, which in turn causes ISC to divide faster and facilitates enteroblast differentiation into new enterocytes.

Epithelial Expression of Apoptotic Proteins Induces ISC Division

We performed a series of experiments to further demonstrate that epithelial damage can indirectly induce ISC division. First, based on microarray expression assays for genes that have high expression in adult gut, we constructed an NPC (Niemann-Pick type C) 1b promoter-Gal4 driver line. Second, we examined the expression after crossing with UAS-GFP, and the GFP signal was clearly seen in the cytoplasm of large-sized enterocytes (arrow, Figures 5N–5Q), but not in nucleus or cytoplasm of small cells (arrowhead). Thus, the NPC1b-Gal4 directs the expression only in mature enterocytes. We then expressed the viral antiapoptotic protein p35 in epithelial cells by NPC1b-Gal4 and performed bleomcyin feeding experiments. The result showed that the bleomycin-induced ISC division is suppressed by 52% (Figure 5R).

Because p35 inhibits caspases (Domingos and Steller, 2007), our result suggests that bleomycin causes DNA damage, triggers caspase activation within the epithelial cells, and somehow stimulates ISC division. Thus, we expressed in epithelial cells the well-established apoptotic inducers Hid and Reaper, which would activate caspases. Such expression caused ISC division to increase by approximately 10-fold, based on phospho-H3 staining (Figure 5S). Overall, our results suggest that epithelial damage by feeding tissue-damaging agents or by expressing apoptotic proteins can trigger a mechanism that ultimately stimulates ISC division.

The Insulin Receptor Signaling Pathway Is Required for Induced ISC Division

We used the inducible ISC division phenotype to examine mutant fly strains and found that insulin receptor (InR) mutants showed a significantly lower number of phospho-H3 positive cells (Figure 6A). The InR mutant also suppressed the DSS and bleomycin-induced cell organization phenotype as revealed by β-catenin staining (Figure 6B–G), probably due to lower ISC division and smaller number of cells in the mutant guts. We examined two other components of the InR signaling pathway. Chico is the *Drosophila* homolog of insulin receptor substrate and the *chico*^{1} mutant showed reduced ISC division (Figure 6A). FOXO is a transcription factor negatively regulated by insulin (Bohni et al., 1999). The FOXO™ transgenic construct contains point mutations at 3 phosphorylation sites that render it constitutively active equal to a loss of insulin regulation (Hwangbo et al., 2004). FOXO™ crossed with esg-Gal4 produced no viable adults; we therefore used the Armadillo-Gal4 driver that has low level ubiquitous expression, and these fly guts showed the predicted phenotype of reduced ISC division (Figure 6A). Thus, three components of the insulin signaling pathway are critical for ISC division.

The MARCM strategy coupled with mutant chromosomes allows positive marking of mutant cell lineage by GFP. Analysis of MARCM flies with *InR* mutant chromosomes revealed that after DSS feeding 90% of GFP-positive clusters contained only 1 or 2 cells (Figure 6H, blank region of the bars, and Figures 6I and 6J), demonstrating a lack of proliferation. In contrast, MARCM flies with wild-type chromosomes had 80% of their GFP-positive clusters contain 3 or more cells (Figure 6H, filled region of the bars). This demonstrates that InR function is required within ISC for proliferation.

We also used various Gal4 drivers to express a constitutively active insulin receptor (InR^{A1325D}) to test in which cell type InR can exert its effect. The esg-Gal4, but not the NPC1b-Gal4, driver led to highly increased ISC division, suggesting that the expression of InR^{A1325D} in precursor cells, but not in epithelial cells, can stimulate ISC division (Figure 6K). Heat shock-induced expression in adult flies also caused a substantial increase in ISC division, demonstrating that InR can regulate ISC division after development has completed. Furthermore, the expression of InR^{A1325D} by the esg-Gal4 driver caused phenotypic changes in the midgut similar to that induced by DSS, including a less organized β-catenin staining pattern (Figures 6L and 6M), clearly stronger Delta staining in ISC (Figures 6N and 6O), and bigger clusters of esg-Gal4/GFP cells (Figures 6P and 6Q). We also performed double staining of phospho-H3 and Delta in guts from flies overexpressing InR^{A1325D} (Figures 6R–6U). 93.0% (n = 499) of the phospho-H3-positive cells also contained Delta staining, demonstrating that it is the stem cells, but not other cells types, that have increased division. Together, the results are consistent with the idea that InR activation leads to ISC proliferation.

Regulation of ISC Division by Systemic Insulin

Drosophila has 7 insulin-like peptides (DILPs), and when expressed by transgenic constructs, all can function to change the growth and metabolic state of the animal (Brogiolo et al., 2001; Ikeya et al., 2002). The main source of DILPs is the median neurosecretory cells in the brain. Ablation of these neurosecretory cells causes insulin depletion phenotypes such as retarded

(Q and R) Clonal analysis by MARCM shows that within one lineage, only one Delta-positive cell is present after bleomycin feeding. For control, see Figure 2P. The arrowheads point to one Delta-positive cell (red) within a GFP-positive cluster. The arrows indicate a bigger cell resembling an enterocyte within the clone.

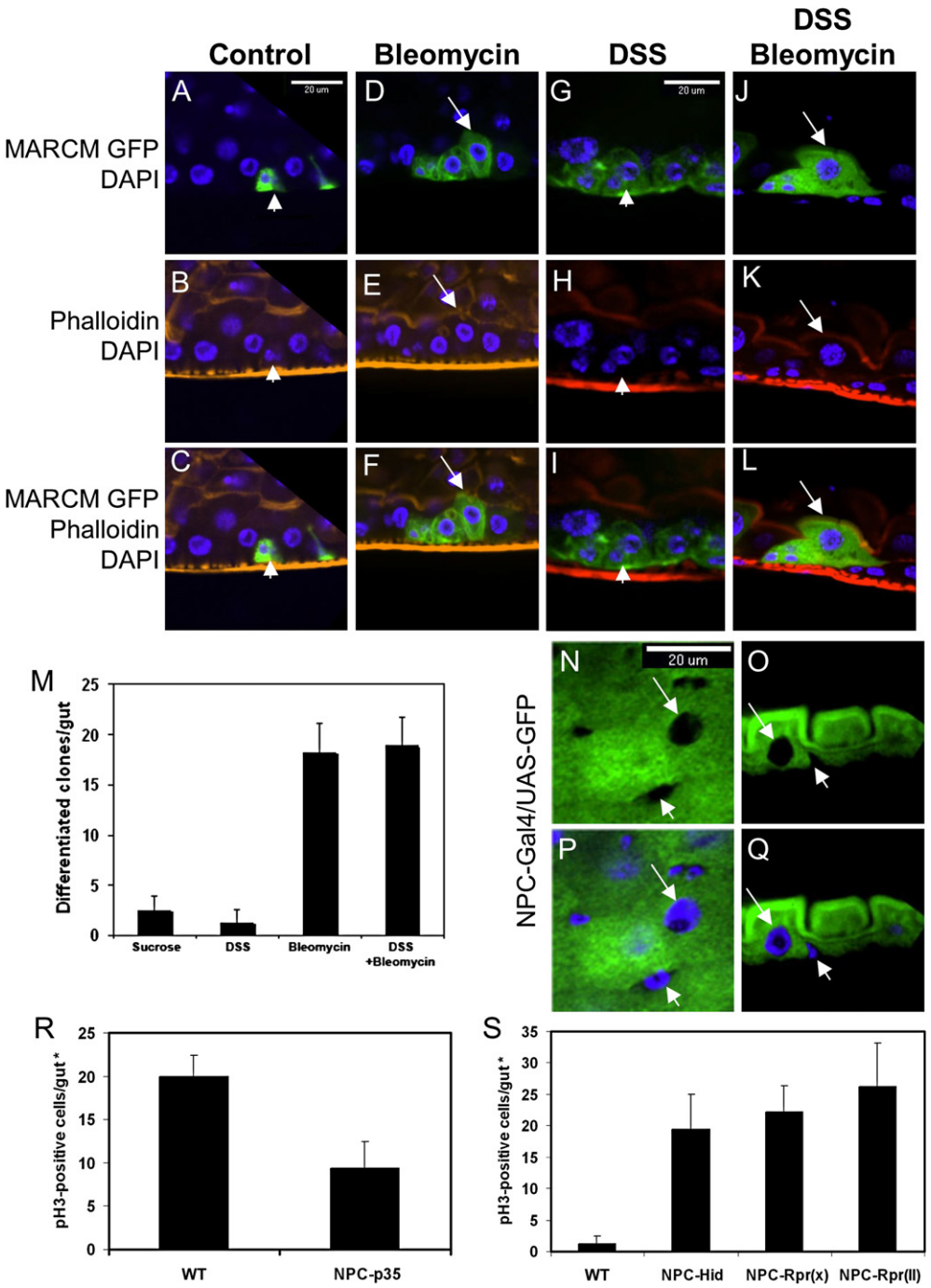

Figure 5. Epithelial Cell Loss Is Coincident with ISC Division and Enteroblast Differentiation

(A–L) All images are sagittal views showing MARCM GFP clusters after feeding with tissue-damaging agents as indicated. In control, the cluster contains two small GFP-positive cells representing ISC and enteroblast (arrowhead). With bleomycin feeding (25 μg/ml), more GFP-positive cells are present in each cluster, and some GFP-positive cells are bigger and have tightly associated phalloidin staining (red) at the apical side, suggesting that they are mature enterocytes (arrow). DSS feeding causes accumulation of enteroblasts that are not associated with phalloidin staining (arrowhead). DSS and bleomycin together causes accumulation of GFP-positive cells as well as bigger cells that have tightly associated phalloidin staining (arrow).

(M) Quantification of the number of MARCM GFP clones that also contained mature cells. Isolated clones were counted from whole guts and only those that contained mature cells are presented in the graph. The result indicates that bleomycin, but not DSS, causes facilitated differentiation. The error bar is standard deviation.

(N–Q) Confocal images of NPC1b-Gal4/UAS-CD8GFP expression in midgut. (N) and (P) are surface views; (O) and (Q) are sagittal views. The arrow indicates lack of GFP signal in an enterocyte nucleus, but enterocyte cytoplasm has strong GFP signal. All small cells do not show GFP signal in both nuclei and cytoplasm (arrowhead).

growth and elevated carbohydrate level (Ikeya et al., 2002; Rulifson et al., 2002). Thus, we performed this ablation experiment by crossing a DILP2-Gal4 driver with UAS-Reaper constructs. Flies containing both DILP2-Gal4 and UAS-Reaper hatched approximately 10 days later than other flies, demonstrating that the ablation caused an insulin depletion phenotype. These flies also showed approximately 90% decrease of DSS-induced and 50% decrease of bleomycin-induced ISC division (Figure 7A). β-catenin staining showed that these DILPs depleted flies, and InR mutant flies had a similar gut phenotype, which means a better organization and smaller number of cells after DSS and bleomycin feeding (Figures 7B–7G). We examined whether this ablation experiment causes a change of gut DILP2 expression. First, we checked the DILP2-Gal4 driven UAS-GFP expression, and we could not observe GFP signal in gut (data not shown). Second, we examined *dilp2* mRNA expression in heads versus guts in the ablated flies and found that the *dilp2* mRNA was largely reduced in heads, while the expression had no change in guts, which was very low to start with (Figure 7H). Third, published papers also show that DILP2 has no expression in the gut (Brogiolo et al., 2001; Ikeya et al., 2002). All these suggest that the ablation experiment mainly affects brain expression. However, there are 7 DILPs in *Drosophila*, and we cannot exclude the possibility that other gene expression is affected. Moreover, ablation of brain cells may indirectly affect gut physiology.

Previous reports show that DILP2 has a consistent effect on growth and metabolism (Brogiolo et al., 2001; Ikeya et al., 2002; Rulifson et al., 2002). Thus, we expressed DILP2 in neurosecretory cells, in gut cells, or ubiquitously by DILP2-Gal4, esg-Gal4, or Armadillo-Gal4, respectively, and examined the effect on ISC proliferation. All these drivers caused approximately 2- to 3-fold increase in phospho-H3-positive cells in the midgut (Figure 7I). This increase is modest but similar to previously reported 2-fold increase in overall growth (Ikeya et al., 2002). Moreover, double staining in DILP2-Gal4/UAS-DILP2 guts showed that 94.0% (n = 134) of the phospho-H3-positive cells also contained Delta staining, demonstrating that it is ISC that have increased division. We conclude that the systemic level of insulin can regulate ISC division in adult midgut.

DISCUSSION

Insulin receptor signaling is essential for cell growth, cell size control, and cell metabolism (Garofalo, 2002; Goberdhan and Wilson, 2003). The function of this pathway, however, has not been reported in any other stem cell systems. We show by various approaches that systemic and gut insulin levels can regulate ISC proliferation, likely by activating InR function within ISC. We propose a model that insulin and other signaling molecules are involved in controlling ISC proliferation and are likely required for intestinal tissue repair (Figure 7J). Depending on whether insulin expression is increased by tissue damage, insulin may act as a permissive or instructive signal to regulate ISC proliferation.

DSS-induced colitis in small experimental mammals is a widely used model for human ulcerative colitis (Kitajima et al., 2000; Rakoff-Nahoum et al., 2004; Tlaskalova-Hogenova et al., 2005; Wirtz et al., 2007). The progression of DSS-induced colitis involves complex interactions of injured tissue with the gut milieu, including B and T lymphocytes and cytokines produced from other cells. *Drosophila* does not have B and T cells, but only hemocytes that function similarly to macrophages and neutrophils (Williams, 2007). Therefore, it is likely that there is no extensive inflammatory reaction in the *Drosophila* midgut, and this may be one of the reasons why we did not observe extensive apoptosis after DSS feeding. The tissue damage in *Drosophila* midgut would then be the primary effect caused by DSS without the complication of lymphocytes, thus representing a simpler model. DSS did not induce proliferation of culture cells (data not shown), and bleomycin-induced DNA damage can lead to cell-cycle arrest (Hagimori et al., 2007). This suggests that ISC are indirectly stimulated by the tissue-damaging effects of DSS and bleomycin.

A powerful role of stem cells in adult tissues is to divide more to help tissue repair. However, adult stem cells may have limited proliferation capacity (Radtke and Clevers, 2005; Wallenfang, 2007). In mammals, ISC division produces progenitor cells that are active in cell division to replenish the different cell types (Crosnier et al., 2006; Walker and Stappenbeck, 2008; Yen and Wright, 2006). A previous report demonstrated that after DSS feeding, mouse intestinal progenitor cells near ulcer regions had increased BrdU incorporation (Pull et al., 2005). However, it is still difficult in mammalian systems to distinguish whether those BrdU-positive cells after tissue injury are only progenitor cells or also include ISC. One reason is that few stem-cell-specific markers are available in mammalian systems, and the exact function of those marked cells is still arguable (Barker et al., 2007; Demidov et al., 2007; He et al., 2007; Scoville et al., 2008; Sangiorgi and Capecchi, 2008). Therefore, our results establish another model system to study ISC-mediated tissue repair.

Stem cell niche is the neighboring environment that helps to maintain stem cell identity and regulates stem cell proliferation (Egger et al., 2008; Kirilly and Xie, 2007; Spradling et al., 2001; Theise, 2006; Wilson and Kotton, 2008). A previous report shows that ISC has a more extensive contact with basement membrane (Ohlstein and Spradling, 2007). Therefore, the disruption of a basement membrane component (collagen IV) by DSS may be sensed by ISC as tissue damage or may affect the niche of ISC. It is also possible that enterocyte loss caused by bleomycin disrupts the contact and releases the inhibition to allow more ISC division. The two mechanisms of niche- and tissue damage-regulated ISC division are not mutually exclusive and can operate at the same time.

(R) Transgenic expression of viral antiapoptotic protein p35 in epithelial cells by NPC1b-Gal4 suppresses approximately 50% of the bleomycin-induced ISC division based on phospho-H3 count. The error bar is standard deviation.

(S) Transgenic expression of apoptotic proteins Hid and Reaper in epithelia cells by NPC1b-Gal4 increases ISC division. Two lines of Reaper, on X and 2nd chromosomes, were used. Phospho-H3-positive cells were counted in guts from 3- to 5-day-old flies. *Note that the NPC-Gal4-driven GFP expression was detected only in the posterior portion of midguts, and we counted phospho-H3-positive cells only in this region rather than in the whole gut, and thus, the overall number of phospho-H3-positive cells was lower than that in other experiments. The error bar is standard deviation.

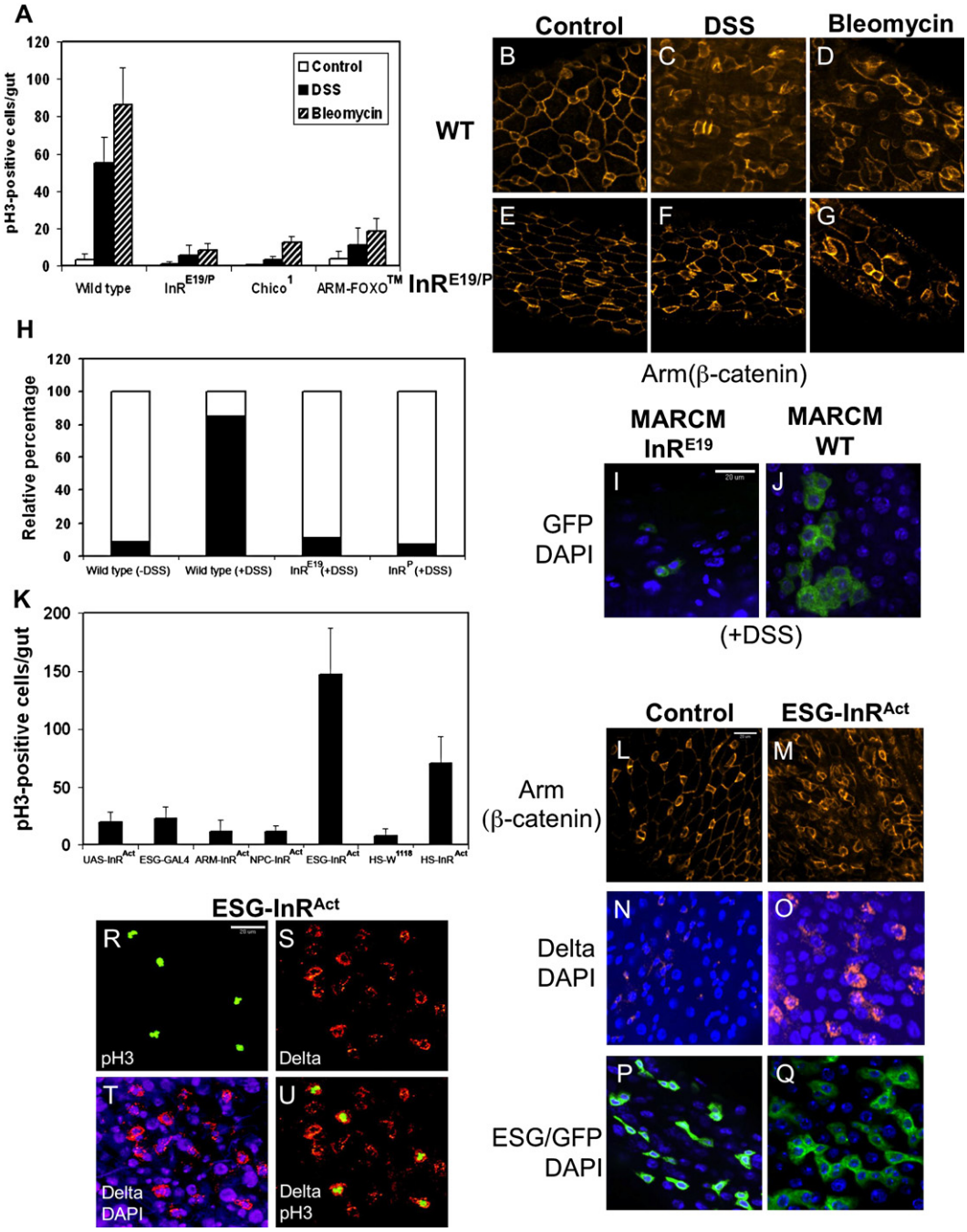

Figure 6. Insulin Receptor Signaling Is Required for ISC Division

(A) Wild-type, *InR*$^{E19/P05545}$ transheterozygotes, *chico*^{1}, and Armadillo-Gal4/UAS-FOXO™ flies were set up for feeding with 3% DSS or 25 μg/ml bleomycin for 2 days. The guts were stained for phospho-H3 and the number of positively stained cells presented. These three fly lines of insulin-signaling components showed significantly reduced ISC division. The error bar is standard deviation.

(B–G) In wild-type guts, Armadillo/β-catenin staining (red) reveals cell membranes of smaller ISC and enteroblasts and of bigger enterocytes. After DSS and bleomycin feeding, the wild-type guts have more small cells and are less organized. InR mutant guts after DSS and bleomycin feeding have fewer small cells, and the organization is more similar to that of control guts.

(H) Quantification of wild-type and InR mutant MARCM GFP clones. The solid portion of each bar represents the percentage of clones with 3 or more cells, and the open portion represents the percentage of clones with 2 or 1 cells. The majority of InR mutant clones had 2 or 1 cells, showing that they had much reduced proliferation. The error bar is standard deviation.

(I and J) Representative images of InR mutant and wild-type MARCM GFP-positive clones after DSS feeding.

(K) Quantification of phospho-H3-positive cells in control and InR^{A1325D}-expressing flies. Armadillo-Gal4, NPC1b-Gal4, esg-Gal4, and heat-shock-Gal4 were used to cross with UAS-InR^{A1325D}. Three- to five-day-old flies from the crosses and various controls were used for gut dissection and phospho-H3 staining. The error bar is standard deviation.

EXPERIMENTAL PROCEDURES

Drosophila Stocks and Feeding Experiments

Information on *Drosophila* genes and stocks is available from Flybase (http://flybase.bio.indiana.edu). y^1w^*, CantonS, and w^{1118} were used as wild-type stocks for gut phenotypic comparison. InR^{E19}, InR^{P05545}, InR^{93Dj-4}, UAS-mCD8GFP, and $chico^1$ were obtained from Bloomington stock center; esg-Gal4 and Su(H)Gbe-lacZ were as described (Micchelli and Perrimon, 2006; Ohlstein and Spradling, 2007); collagenIV-GFP (G454) was obtained from FlyTrap collection; and UAS-InR^{A1325D} was as described (Flybase FBal0156362). The following stocks were generous gifts: UAS-hid and UAS-reaper from John Abrams, UAS-p35 from Michael Brodsky, UAS-FOXO™ from Marc Tatar, and DILP2Gal4 and UAS-DILPs from Ping Shen. Flies were maintained on cornmeal-yeast-molasses-agar media. Stocks were kept at room temperature. For viability tests and feeding experiments, the flies were kept at 29°C. We observed a faster appearance of the gut phenotype in this temperature; lower temperature of incubation also showed the phenotypes but took longer time. The MARCM flies were grown at 18°C, and the feeding experiments with these flies were performed at 18°C. It took approximately 14 days for the tissue damage-induced proliferation to occur at 18°C; higher temperature of incubation resulted in faster appearance of phenotype.

For viability tests, we consistently used 50–100 flies per vial. For gut phenotype induction, the number of flies used was 10–100 in each vial, depending on the availability of the strain. The phenotypes were reproducible regardless of the number of flies used. Feeding experiments involved using 3–5 day old flies in an empty vial containing a piece of 2.5 cm × 3.75 cm chromatography paper (Fisher). 500 μl of 5% sucrose solution was used to wet the paper as feeding medium. The chemicals included in the feeding medium were 1%–5% of dextran sulfate sodium (MP Biomedicals) as indicated in the figure, 3% heparin (Sigma), 3% dextran (MP Biomedicals), 25 μg/ml bleomycin (Sigma), or as indicated in the figure. Flies that were still alive were transferred to new vials with fresh feeding media every day. Most feeding experiments were performed for 2 days at 29°C or as specified in the figure legend.

For lineage analysis, GFP-marked intestinal stem cell clones from MARCM were generated as previously described (Lee and Luo, 2001). Briefly, flies stocks were crossed to generate offspring with the genotype: hsFLP; FRTG13 UAS-CD8GFP/FRTG13 tubulin-Gal80; and tubulin Gal4/+. The final cross and offspring were maintained at 18°C. These stocks at the 18°C incubation temperature generated small number of GFP-positive mitotic clones in midgut without heat shock induction of the FLP recombinase. Only flies that had all the correct chromosomes exhibited this low level of mitotic recombination, and the GFP-marked ISC grew to include bigger cells, as observed in older flies. These are consistent with having successful mitotic recombination, which, by chance, eliminates the repressor Gal80 in a mitotic stem cell and allows Gal4-driven GFP to be expressed within the lineage. For tissue damage experiments, these flies were set up for feeding in 18°C for 7–14 days before dissecting guts for staining with antibody.

Immunostaining and Fluorescent Microscopy

For gut dissection, female flies were used routinely because of the bigger size, but male flies were also used to check the phenotypes. The entire gastrointestinal tract was pulled from the posterior end directly into fixation medium containing 1× PBS and 4% Formaldehyde (Mallinckrodt Chemicals). Guts were fixed in this medium for 3 hr, except for Delta staining where the fixation was for 0.5 hr. Subsequent rinses, washes, and incubations with primary and secondary antibodies were done in a solution containing 1× PBS, 0.5% BSA, and 0.1% Triton X-100. The following anti-sera were used: anti-Delta (monoclonal 1:100 dilution), anti-Prospero (monoclonal 1:50 dilution), and anti-Spectrin (monoclonal 1:100 dilution) (all from Developmental Studies Hybridoma Bank); anti-phospho-histone H3 (rabbit 1:2000 dilution) (Upstate Biotechnology); anti-βGal (monoclonal 1:500 dilution) (Promega); anti-bGal (rabbit 1:1000, preabsorbed against fixed midguts) (Cappel, MP Biomedicals); and anti-H2AvD (rabbit 1:1000 dilution) (Rockland). Secondary antibodies were used in 1:2000 dilution as follows: goat anti-mouse IgG conjugated to either Alexa 488 or Alexa 568, and goat anti-rabbit IgG conjugated to either Alexa 488 or Alexa 546 (Molecular probes). DAPI (Vectorshield, Vector Lab) was used at 0.75 mg/ml. Images were taken by a Nikon Spinning Disk confocal microscope (UMass Medical School Imaging Core Facility).

ACKNOWLEDGMENTS

We thank Tzumin Lee for MARCM flies, Bill Theurkauf for H2AvD antibody, Ping Shen for DILP flies, and Lynn Cooley for collagen IV-GFP flies originated from Bill Chia. We also thank Michael Brodsky, John Abrams, Marc Tatar, Norbert Perrimon, and Allan Spradling for sharing fly stocks. The work in YTI laboratory was supported by grants from NIH (DK75545 and GM53269) and Worcester Foundation for Biomedical Research. The work in J.J.'s laboratory was supported by grants from NIH, Welch Foundation, and Leukemia and Lymphoma Society. Core resources supported by the Diabetes Endocrinology Research Center grant DK32520 were also used.

Received: March 7, 2008
Revised: August 12, 2008
Accepted: October 27, 2008
Published: January 8, 2009

REFERENCES

Baba, Y., Iyama, K., Ikeda, K., Ishikawa, S., Hayashi, N., Miyanari, N., Honda, Y., Sado, Y., Ninomiya, Y., and Baba, H. (2007). Differential expression of basement membrane type IV collagen alpha chains in gastric intramucosal neoplastic lesions. J. Gastroenterol. *42*, 874–880.

Barker, N., van Es, J.H., Kuipers, J., Kujala, P., van den Born, M., Cozijnsen, M., Haegebarth, A., Korving, J., Begthel, H., Peters, P.J., and Clevers, H. (2007). Identification of stem cells in small intestine and colon by marker gene Lgr5. Nature *449*, 1003–1007.

Bohni, R., Riesgo-Escovar, J., Oldham, S., Brogiolo, W., Stocker, H., Andruss, B.F., Beckingham, K., and Hafen, E. (1999). Autonomous control of cell and organ size by CHICO, a *Drosophila* homolog of vertebrate IRS1–4. Cell *97*, 865–875.

Bray, S. (2006). Notch signalling: a simple pathway becomes complex. Nat. Rev. Mol. Cell Biol. *7*, 678–689.

Brogiolo, W., Stocker, H., Ikeya, T., Rintelen, F., Fernandez, R., and Hafen, E. (2001). An evolutionarily conserved function of the *Drosophila* insulin receptor and insulin-like peptides in growth control. Curr. Biol. *11*, 213–221.

Choi, N.H., Kim, J.G., Yang, D.J., Kim, Y.S., and Yoo, M.A. (2008). Age-related changes in *Drosophila* midgut are associated with PVF2, a PDGF/VEGF-like growth factor. Aging Cell *7*, 318–334.

Clarkson, M.J., Wells, J.R., Gibson, F., Saint, R., and Tremethick, D.J. (1999). Regions of variant histone His2AvD required for *Drosophila* development. Nature *399*, 694–697.

Crosnier, C., Stamataki, D., and Lewis, J. (2006). Organizing cell renewal in the intestine: stem cells, signals and combinatorial control. Nat. Rev. Genet. *7*, 349–359.

Demidov, O.N., Timofeev, O., Lwin, H.N., Kek, C., Appella, E., and Bulavin, D.V. (2007). Wip1 phosphatase regulates p53-dependent apoptosis of stem cells and tumorigenesis in the mouse intestine. Cell Stem Cell *1*, 180–190.

Domingos, P.M., and Steller, H. (2007). Pathways regulating apoptosis during patterning and development. Curr. Opin. Genet. Dev. *17*, 294–299.

(L–Q) Cellular phenotypes in midgut induced by esg-Gal4/UAS-InR^{A1325D}. Armadillo/β-catenin staining shows that there are more small cells, and the overall arrangement appears more disorganized. The Delta staining is more prominent in ISC of esg-Gal4/UAS-InR^{A1325D} flies. There are also more esg-Gal4/UAS-CD8GFP-positive cells.

(R–U) Colocalization of phospho-H3-positive cells with the ISC marker Delta in the gut of esg-Gal4/UAS-InR^{A1325D} flies. 93.0% (n = 499) of the phospho-H3-positive cells also contained Delta staining.

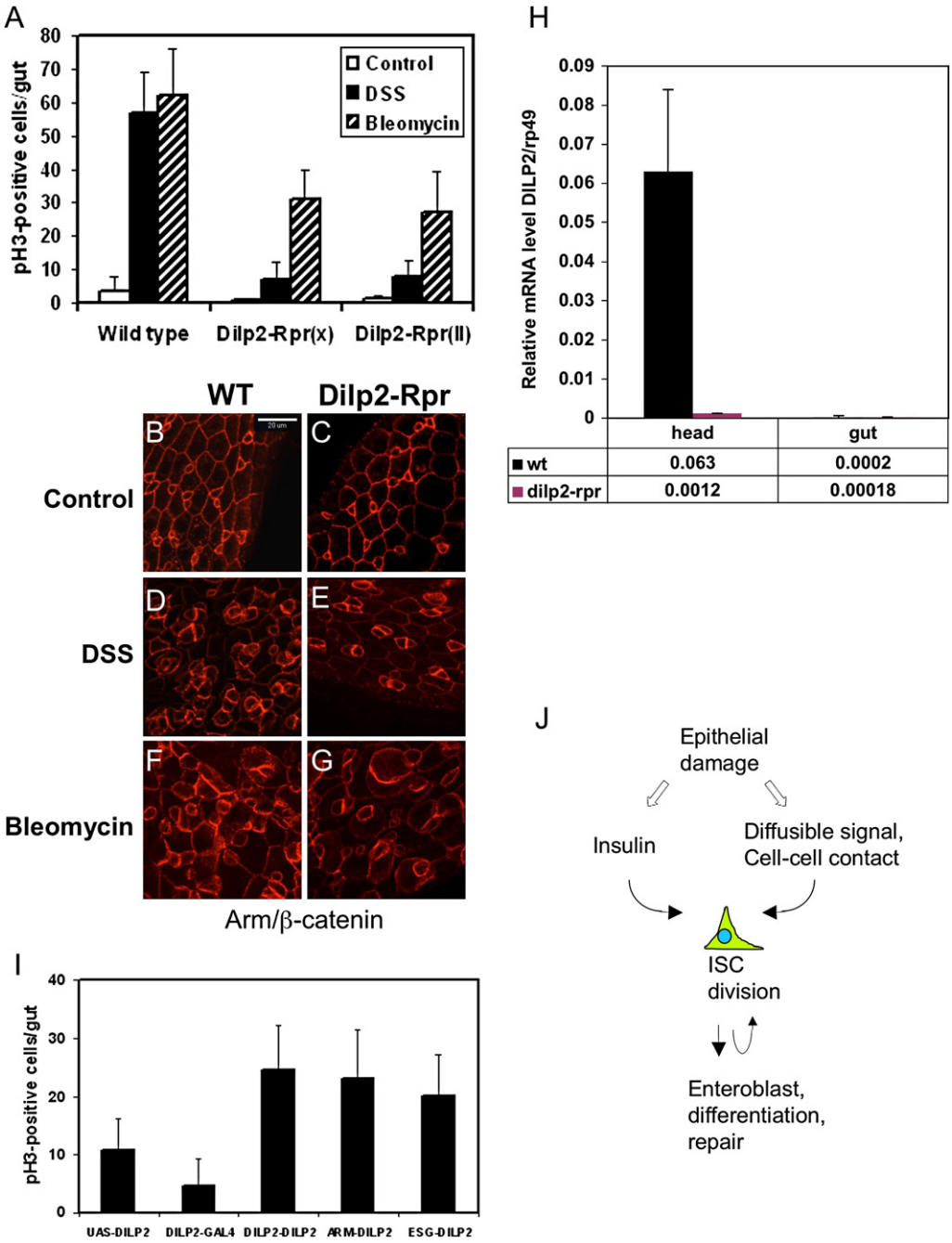

Figure 7. Systemic Insulin Level Can Regulate ISC Division

(A) Quantification of phospho-H3-positive cells in gut after insulin neurosecretory cell ablation. Two different transgenic lines of UAS-Reaper (Rpr, on X and 2nd chromosome) were crossed with DILP2-Gal4. These Reaper-expressing flies showed approximately 10 days delay of hatching. These flies were used for 3% DSS and 25 μg/ml bleomycin feeding experiments for 2 days. Control was 5% sucrose alone. There was approximately 85% reduction for DSS- and 50% reduction for bleomycin-induced ISC division. The error bar is standard deviation.

(B–G) Armadillo/β-catenin staining of DILP2-Gal4/UAS-Reaper fly guts. The wild-type guts have more small cells and disorganized after DSS and bleomycin feeding, while the Dilp2-Rpr fly guts have fewer cells and appear more organized, similar to that of InR mutant.

(H) Quantification of *dilp2* mRNA expression in heads and guts. The RT-PCR cycle numbers at log phase of *dilp2* and *rp49* from wild-type and DILP2-Gal4/UAS-Reaper were used to calculate the relative expression level $1/(2^{cy\#a-cy\#rp49})$. The expression level of *rp49* is 1. The error bar is standard deviation.

(I) DILP2-, Armadillo-, and esg-Gal4 driver lines were crossed with UAS-DILP2, and the parental UAS-DILP2 and DILP2-Gal4 were included as controls. Three- to five-day-old flies from the crosses were assayed for phospho-H3 staining in the guts. Transgenic expression of DILP2 in various tissues causes a similar increase in ISC division. The error bar is standard deviation.

(J) A model for regulation of ISC division. The systemic level of insulin can regulate InR signaling in ISC to control proliferation. Damaged epithelium may release other signals, or change cell-cell contacts, that cooperate with insulin signaling to increase ISC division and subsequent enteroblast differentiation for tissue repair.

Egger, B., Chell, J.M., and Brand, A.H. (2008). Insights into neural stem cell biology from flies. Philos. Trans. R. Soc. Lond. B Biol. Sci. *363*, 39–56.

Fodde, R., and Brabletz, T. (2007). Wnt/beta-catenin signaling in cancer stemness and malignant behavior. Curr. Opin. Cell Biol. *19*, 150–158.

Garofalo, R.S. (2002). Genetic analysis of insulin signaling in *Drosophila*. Trends Endocrinol. Metab. *13*, 156–162.

Goberdhan, D.C., and Wilson, C. (2003). The functions of insulin signaling: size isn't everything, even in *Drosophila*. Differentiation *71*, 375–397.

Hagimori, K., Fukuda, T., Hasegawa, Y., Omura, S., and Tomoda, H. (2007). Fungal malformins inhibit bleomycin-induced G2 checkpoint in Jurkat cells. Biol. Pharm. Bull. *30*, 1379–1383.

He, X.C., Yin, T., Grindley, J.C., Tian, Q., Sato, T., Tao, W.A., Dirisina, R., Porter-Westpfahl, K.S., Hembree, M., Johnson, T., et al. (2007). PTEN-deficient intestinal stem cells initiate intestinal polyposis. Nat. Genet. *39*, 189–198.

Hwangbo, D.S., Gershman, B., Tu, M.P., Palmer, M., and Tatar, M. (2004). *Drosophila* dFOXO controls lifespan and regulates insulin signalling in brain and fat body. Nature *429*, 562–566.

Ikeya, T., Galic, M., Belawat, P., Nairz, K., and Hafen, E. (2002). Nutrient-dependent expression of insulin-like peptides from neuroendocrine cells in the CNS contributes to growth regulation in *Drosophila*. Curr. Biol. *12*, 1293–1300.

Kawada, M., Arihiro, A., and Mizoguchi, E. (2007). Insights from advances in research of chemically induced experimental models of human inflammatory bowel disease. World J. Gastroenterol. *13*, 5581–5593.

Kirilly, D., and Xie, T. (2007). The *Drosophila* ovary: an active stem cell community. Cell Res. *17*, 15–25.

Kitajima, S., Takuma, S., and Morimoto, M. (2000). Histological analysis of murine colitis induced by dextran sulfate sodium of different molecular weights. Exp. Anim. *49*, 9–15.

Klattenhoff, C., Bratu, D.P., McGinnis-Schultz, N., Koppetsch, B.S., Cook, H.A., and Theurkauf, W.E. (2007). *Drosophila* rasiRNA pathway mutations disrupt embryonic axis specification through activation of an ATR/Chk2 DNA damage response. Dev. Cell *12*, 45–55.

LeBleu, V.S., Macdonald, B., and Kalluri, R. (2007). Structure and function of basement membranes. Exp. Biol. Med. (Maywood) *232*, 1121–1129.

Lee, T., and Luo, L. (2001). Mosaic analysis with a repressible cell marker (MARCM) for *Drosophila* neural development. Trends Neurosci. *24*, 251–254.

Metcalfe, A.D., and Ferguson, M.W. (2008). Molecular and Cellular Basis of Regeneration and Tissue Repair: Skin stem and progenitor cells: using regeneration as a tissue-engineering strategy. Cell. Mol. Life Sci. *65*, 24–32.

Micchelli, C.A., and Perrimon, N. (2006). Evidence that stem cells reside in the adult *Drosophila* midgut epithelium. Nature *439*, 475–479.

Morel, F., Renoux, M., Lachaume, P., and Alziari, S. (2008). Bleomycin-induced double-strand breaks in mitochondrial DNA of *Drosophila* cells are repaired. Mutat. Res. *637*, 111–117.

Nakamura, T., Tsuchiya, K., and Watanabe, M. (2007). Crosstalk between Wnt and Notch signaling in intestinal epithelial cell fate decision. J. Gastroenterol. *42*, 705–710.

Niemeyer, P., Krause, U., Kasten, P., Kreuz, P.C., Henle, P., Sudkam, N.P., and Mehlhorn, A. (2006). Mesenchymal stem cell-based HLA-independent cell therapy for tissue engineering of bone and cartilage. Curr. Stem Cell Res. Ther. *1*, 21–27.

Nystul, T.G., and Spradling, A.C. (2006). Breaking out of the mold: diversity within adult stem cells and their niches. Curr. Opin. Genet. Dev. *16*, 463–468.

Ohlstein, B., and Spradling, A. (2006). The adult *Drosophila* posterior midgut is maintained by pluripotent stem cells. Nature *439*, 470–474.

Ohlstein, B., and Spradling, A. (2007). Multipotent *Drosophila* intestinal stem cells specify daughter cell fates by differential notch signaling. Science *315*, 988–992.

Pull, S.L., Doherty, J.M., Mills, J.C., Gordon, J.I., and Stappenbeck, T.S. (2005). Activated macrophages are an adaptive element of the colonic epithelial progenitor niche necessary for regenerative responses to injury. Proc. Natl. Acad. Sci. USA *102*, 99–104.

Radtke, F., and Clevers, H. (2005). Self-renewal and cancer of the gut: two sides of a coin. Science *307*, 1904–1909.

Rakoff-Nahoum, S., Paglino, J., Eslami-Varzaneh, F., Edberg, S., and Medzhitov, R. (2004). Recognition of commensal microflora by toll-like receptors is required for intestinal homeostasis. Cell *118*, 229–241.

Rulifson, E.J., Kim, S.K., and Nusse, R. (2002). Ablation of insulin-producing neurons in flies: growth and diabetic phenotypes. Science *296*, 1118–1120.

Sangiorgi, E., and Capecchi, M.R. (2008). Bmi1 is expressed in vivo in intestinal stem cells. Nat. Genet. *40*, 915–920.

Scoville, D.H., Sato, T., He, X.C., and Li, L. (2008). Current view: intestinal stem cells and signaling. Gastroenterology *134*, 849–864.

Spradling, A., Drummond-Barbosa, D., and Kai, T. (2001). Stem cells find their niche. Nature *414*, 98–104.

Takada, S., Kelkar, A., and Theurkauf, W.E. (2003). *Drosophila* checkpoint kinase 2 couples centrosome function and spindle assembly to genomic integrity. Cell *113*, 87–99.

Theise, N.D. (2006). The stem cell niche and tissue biology. Stem Cell Rev. *2*, 169–170.

Tlaskalova-Hogenova, H., Tuckova, L., Stepankova, R., Hudcovic, T., Palova-Jelinkova, L., Kozakova, H., Rossmann, P., Sanchez, D., Cinova, J., Hrncir, T., et al. (2005). Involvement of innate immunity in the development of inflammatory and autoimmune diseases. Ann. N Y Acad. Sci. *1051*, 787–798.

Walker, M., and Stappenbeck, T. (2008). Deciphering the 'black box' of the intestinal stem cell niche: taking direction from other systems. Curr. Opin. Gastroenterol. *24*, 115–120.

Wallenfang, M.R. (2007). Aging within the Stem Cell niche. Dev. Cell *13*, 603–604.

Williams, M.J. (2007). *Drosophila* hemopoiesis and cellular immunity. J. Immunol. *178*, 4711–4716.

Wilson, A.A., and Kotton, D.N. (2008). Another notch in stem cell biology: *Drosophila* intestinal stem cells and the specification of cell fates. Bioessays *30*, 107–109.

Wirtz, S., Neufert, C., Weigmann, B., and Neurath, M.F. (2007). Chemically induced mouse models of intestinal inflammation. Nat. Protocols *2*, 541–546.

Yen, T.H., and Wright, N.A. (2006). The gastrointestinal tract stem cell niche. Stem Cell Rev. *2*, 203–212.